

# Differential olivo-cerebellar cortical control of rebound activity in the cerebellar nuclei

Freek E. Hoebeek<sup>a,1</sup>, Laurens Witter<sup>b,1</sup>, Tom J. H. Ruigrok<sup>a,1</sup>, and Chris I. De Zeeuw<sup>a,b,2</sup>

<sup>a</sup>Department of Neuroscience, Erasmus Medical Center, 3000 CA, Rotterdam, The Netherlands; and <sup>b</sup>Netherlands Institute for Neuroscience, Royal Academy for Arts and Sciences, 1105 BA, Amsterdam, The Netherlands

Edited\* by Rodolfo R. Llinas, New York University Medical Center, New York, NY, and approved March 15, 2010 (received for review June 28, 2009)

**The output of the cerebellar cortex is controlled by two main inputs, (i.e., the climbing fiber and mossy fiber-parallel fiber pathway) and activations of these inputs elicit characteristic effects in its Purkinje cells: that is, the so-called complex spikes and simple spikes. Target neurons of the Purkinje cells in the cerebellar nuclei show rebound firing, which has been implicated in the processing and storage of motor coordination signals. Yet, it is not known to what extent these rebound phenomena depend on different modes of Purkinje cell activation. Using extracellular as well as patch-clamp recordings, we show here in both anesthetized and awake rodents that simple and complex spike-like train stimuli to the cerebellar cortex, as well as direct activation of the inferior olive, all result in rebound increases of the firing frequencies of cerebellar nuclei neurons for up to 250 ms, whereas single-pulse stimuli to the cerebellar cortex predominantly elicit well-timed spiking activity without changing the firing frequency of cerebellar nuclei neurons. We conclude that the rebound phenomenon offers a rich and powerful mechanism for cerebellar nuclei neurons, which should allow them to differentially process the climbing fiber and mossy fiber inputs in a physiologically operating cerebellum.**

olivo-cerebellar loop | rebound firing | Purkinje cell | complex spikes | simple spikes

Neurons in the cerebellar nuclei (CN) form the main output of the cerebellum (1). They include GABAergic neurons that provide an inhibitory feedback to the inferior olive (IO) and excitatory neurons that project to various other brainstem nuclei exerting motor control (2–4). In turn, each CN neuron receives a prominent inhibitory GABAergic input from tens of Purkinje cells, a substantial excitatory input from climbing fiber and mossy fiber collaterals, and a modest input from the local interneurons (4–7). Apart from the impact of these inputs, the firing pattern of CN neurons is largely determined by their intrinsic activities (4, 8–14). Interestingly, following inhibitory current injections or activation of their Purkinje cell input, CN neurons can show a “rebound” depolarization of the membrane potential, accompanied by action-potential firing (8, 11). Even though little is known about the prominence of rebound firing in the awake state, various models on cerebellar function consider this rebound phenomenon in the nuclei as an essential mechanism to process and store relevant information on motor coordination (15–18). The conductances that allow the rebound firing to emerge involve various types of Ca<sup>2+</sup>-channels, the distribution of which probably varies among the different types of neurons in the CN (8, 11, 14, 19–23). Regardless of the type of CN neuron, it is tempting to hypothesize that the climbing fibers and parallel fibers, which evoke complex spikes and simple spikes (24–27), respectively, have a differential impact on the generation of rebound activities in the CN neurons.

To test this hypothesis, we recorded spike patterns of CN neurons in rodents, while applying simple spike-like, single-pulse stimuli or complex spike-like, high-frequency train stimuli to the cerebellar cortex or IO. To subsequently identify the nature and source of these responses, we used in vivo whole-cell patch-clamp recordings. We conclude that single-pulse stimuli to the cerebellar cortex mostly elicit well-timed spiking activity in CN neurons

without altering the average firing frequency, whereas both simple spike-like and complex spike-like train stimuli or activation of the IO additionally result in increases in firing frequency.

## Results

### Rebound Activity in Cerebellar Nuclei of Awake, Behaving Animals.

To investigate the prevalence of rebound firing in CN neurons under physiological circumstances, we recorded single-unit activity patterns in the interposed nuclei of awake, behaving mice while electrically stimulating the paravermal region of lobules VI/VII. Overall, the spontaneous activity of the 50 recorded CN neurons varied substantially, as indicated by the wide range of frequencies and coefficient of variance 1 and 2 values (Fig. S1). We found that 27 of the 50 CN neurons responded with a pause in their firing to a train stimulus (10 pulses at 100 Hz; 100–300  $\mu$ A) that mimics near-maximal in vivo Purkinje cell simple-spike activity (19, 28, 29). To compare the responses to this simple spike-like stimulation between individual neurons, we normalized the firing frequencies to the mean values during the last and first six interspike intervals (ISIs) before and after the stimulus, respectively (Fig. 1A). This analysis revealed that the average firing frequency during the first six ISIs poststimulus was significantly ( $P < 0.05$ ) increased (up to 190 Hz) in 15 (56%) of the 27 responsive CN neurons by an average of  $42.8 \pm 8.5\%$ ; however, 8 neurons showed no change ( $1.2 \pm 1.2\%$ ) and 4 neurons reduced their firing frequency ( $-20.9 \pm 7.7\%$ ) (Fig. 1A and B).

Calculating the average firing frequency over a fixed number of ISIs (see also refs. 19 and 28), however, does not provide information on the exact timing of the spiking activity in CN neurons and assumes a minimal length for rebound responses (e.g., see ref. 30). To analyze the exact time point at which the chance of spiking is increased, we adapted a convolution method that reforms spiking patterns into a normalized chance of spiking (modified from ref. 31) by replacing each spike in the raster plots with a 1-ms SD Gaussian distribution and summing the results over trials (for detailed explanation see *SI Materials and Methods* and Fig. S2). The resulting arbitrary units indicate the normalized chance of spiking and form a measure of spike precision. Stretches with a significant deviation ( $\pm 3$  SD) from the mean normalized spiking chance reflect in or decreases in the relative chance of firing a spike during that period relative to the stimulus. For such increases in the chance of firing a spike, we propose the term “timed-spiking” (Fig. 1C). We found that 20 (74%) of the 27 responsive neurons showed timed-spiking activity during  $20.3 \pm 4.2$  ms (range 1.0–58.1 ms)

Author contributions: F.E.H., L.W., T.J.H.R., and C.I.D.Z. designed research; F.E.H., L.W., and T.J.H.R. performed research; F.E.H., L.W., and T.J.H.R. analyzed data; and F.E.H., L.W., T.J.H.R., and C.I.D.Z. wrote the paper.

The authors declare no conflict of interest.

\*This Direct Submission article had a prearranged editor.

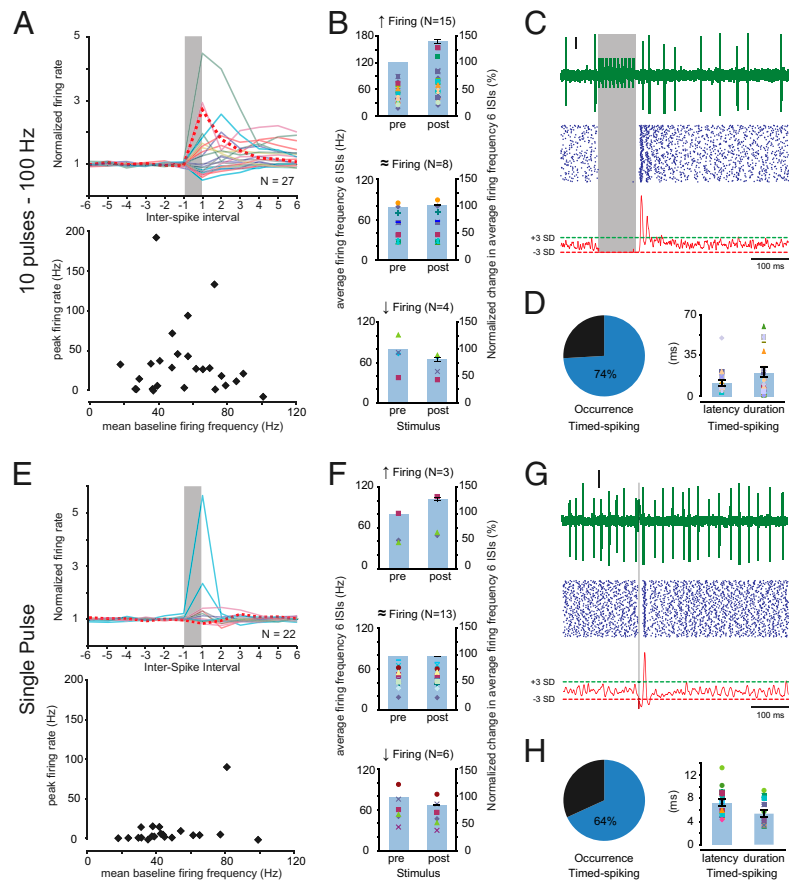
Freely available online through the PNAS open access option.

<sup>1</sup>F.E.H., L.W., and T.J.H.R. contributed equally to this work.

<sup>2</sup>To whom correspondence should be addressed. E-mail: c.dezeeuw@erasmusmc.nl.

This article contains supporting information online at [www.pnas.org/cgi/content/full/0907118107/DCSupplemental](http://www.pnas.org/cgi/content/full/0907118107/DCSupplemental).

**Fig. 1.** Extracellular recordings in CN neurons of awake mice. (A) Responses in the interposed nuclei to stimulation of the paravermal lobules VI/VII with a 100-Hz train of 10 pulses (each pulse 80  $\mu$ s, 100–300  $\mu$ A). (Upper) Instantaneous firing rate for the last six ISIs before the stimulus (prestimulus) and six ISIs after the stimulus-induced pause in firing (poststimulus) normalized to the average prestimulus firing frequency. The vertical gray bar (nonscaled) indicates the stimulus and each colored line represents data of an individual cell. The striped, bold, red line indicates data of the typical example in C. (Lower) Peak firing rate during the first six ISIs poststimulus represents the maximum firing frequency beyond the mean baseline firing frequency. (B) The scatter plots (left vertical axes) indicate the average firing frequencies during the last six ISIs prestimulus (Left) and the first six ISIs poststimulus (Right). Each marker indicates data from a single neuron. Bar plots (right vertical axes) indicate the change in average firing frequencies normalized to the mean prestimulus firing frequency. Data in B is grouped by significance of the changes (tested by ANOVA; *SI Materials and Methods*) in firing frequency. (Top) Fifteen CN neurons showed a significant increase in firing frequency. (Middle) Eight CN neurons showed no significant change in firing frequency. (Bottom) Four CN neurons showed a significant decrease in firing frequency. (C) (Top) Individual trace of CN activity with truncated stimulus artifacts. Vertical scale bar indicates 10  $\mu$ V. (Middle) Accompanying raster plot of 100 repeats. (Bottom) Gaussian-convolved spiking chance (see main text, *SI Materials and Methods*, and Fig. S2 for detailed description). Red and green dashed lines indicate the  $-3$  SD and  $+3$  SD thresholds, respectively; crossings with the green dashed line ( $+3$  SD) indicates a significantly ( $P < 0.001$ ) increased chance of spiking (e.g., timed-spiking). (D) (Left) Pie-chart indicating that 20 out of 27 responsive CN neurons showed timed-spiking in response to a 10 pulses/100 Hz stimulus. (Right) Scatter plots indicate the latency (Left) and duration (Right) of episode of timed-spiking per neuron, and Bar plots indicate the averages. (E–H) As in A to D, using a single-pulse (80  $\mu$ s, 100–300  $\mu$ A) stimulus. (E) (Upper) Normalized and (Lower) peak firing rates of CN neurons ( $n = 22$ ) responded less to a single-pulse stimulus than to a 10-pulses at 100-Hz stimulus train. (F) (Top) Three CN neurons showed significantly increased average firing frequencies during the six ISIs poststimulus compared with the six ISIs prestimulus. (Middle) Thirteen CN neurons showed no significant change. (Bottom) Six CN neurons showed significantly reduced firing frequencies. (G and H) Note the consistent prevalence of timed-spiking activity in response to the single-pulse stimuli.



following an initial latency (relative to the end of the stimulus) of  $9.7 \pm 1.2$  ms (range 4.1–21.8 ms) (Fig. 1D).

Next, we wondered whether single-pulse stimuli could evoke similar rebound activities. Single-pulse stimuli of 80  $\mu$ s failed to induce changes in the firing rate of most neurons (Fig. 1E); only 3 of the 22 (14%) responsive CN neurons showed a significant ( $P < 0.05$ ) increase of  $28.7 \pm 6.7\%$  in their poststimulus firing frequency; 13 (59%) showed no change ( $-0.9 \pm 0.8\%$ ), and 6 (27%) showed a significant reduction ( $-13.5 \pm 2.7\%$ ;  $P < 0.05$ ) (Fig. 1F). However, when we analyzed the timed-spiking activity, 14 (64%) showed an increased chance of spiking for  $5.1 \pm 0.5$  ms (range 2.9–8.5 ms) (Fig. 1G and H). Although the initial latency of this well-timed spiking response ( $8.0 \pm 0.6$  ms; range 5.3–14.2 ms) was equally short as with train stimuli ( $P = 0.24$ ), the average duration was significantly shorter ( $P < 0.005$ ). Thus, our data indicate that single-pulse stimuli predominantly induced timed-spiking activity without changing the average firing frequency, whereas simple spike-like train stimuli additionally induced increased firing frequencies.

#### Negative Shift Action-Potential Threshold Induces Timed-Spiking That Precedes Rebound Depolarization-Induced Increased Firing Frequency.

To elucidate whether both the increased firing frequency and timed-spiking activity are accompanied by rebound depolarizations of the membrane potential ( $V_m$ ), we performed whole-cell patch-clamp recordings in vivo in the interposed nuclei of anesthetized mice while stimulating the paravermis of lobules VI/VII ( $n = 20$ ). We used ketamine/xylazine and not isoflurane to sedate the mice, because isoflurane directly hampers the occurrence of rebound activity as this anesthetic affects various voltage-gated ion channels

(19, 21, 28, 32, 33) (Fig. S3), whereas ketamine/xylazine blocks  $\alpha 6$ - and  $\delta$ -subunit containing GABA<sub>A</sub>-receptors (34), which are at most sparsely present in the CN (35, 36) (see also ref. 37 for other effects).

When stimulating the cerebellar cortex with 10 pulses at 100 Hz ( $n = 10$ ), the  $V_m$  of all CN neurons dropped to more hyperpolarized levels ( $-12.5 \pm 4.9$  mV) relative to the resting  $V_m$  ( $-52.0 \pm 1.2$  mV) (Fig. 2A and B and Fig. S4). Following this “hyperpolarization,” 6 of the 10 responsive neurons showed a significant “depolarization” of  $1.5 \pm 0.3$  mV (Fig. 2B) (see *SI Materials and Methods*). The occurrence of this depolarization was indeed accompanied by a significant increase in the poststimulus firing frequency ( $n = 5$ ). Moreover, these intracellular recordings showed that most (60%) of the 10 responsive CN neurons showed a period during which the chance of spiking was significantly increased. Interestingly, however, the timed-spiking responses in these six neurons appeared before the significant rebound depolarization (Fig. 2A). In search of an explanation for this result, we studied the kinetics of these timed action potentials and found their initiation threshold to be more negative (Fig. 2C). Similarly, single-pulse stimuli applied to the cerebellar cortex consistently resulted initially in a hyperpolarized membrane potential ( $V_m$ ) ( $-4.6 \pm 0.6$  mV relative to resting  $V_m$  of  $-54.1 \pm 1.8$  mV) in all 20 CN neurons, which was followed by a significant depolarization ( $1.1 \pm 0.2$  mV) in 9 of these neurons (Fig. 2D and E). During this rebound depolarization six of these nine neurons showed an increased firing frequency. When we analyzed the timed-spiking activity to such single-pulse stimuli, 12 of the 20 responsive CN neurons showed a significantly increased chance of firing action potentials, which occurred before the membrane depolarization and showed lower initiation thresholds (Fig. 2F).

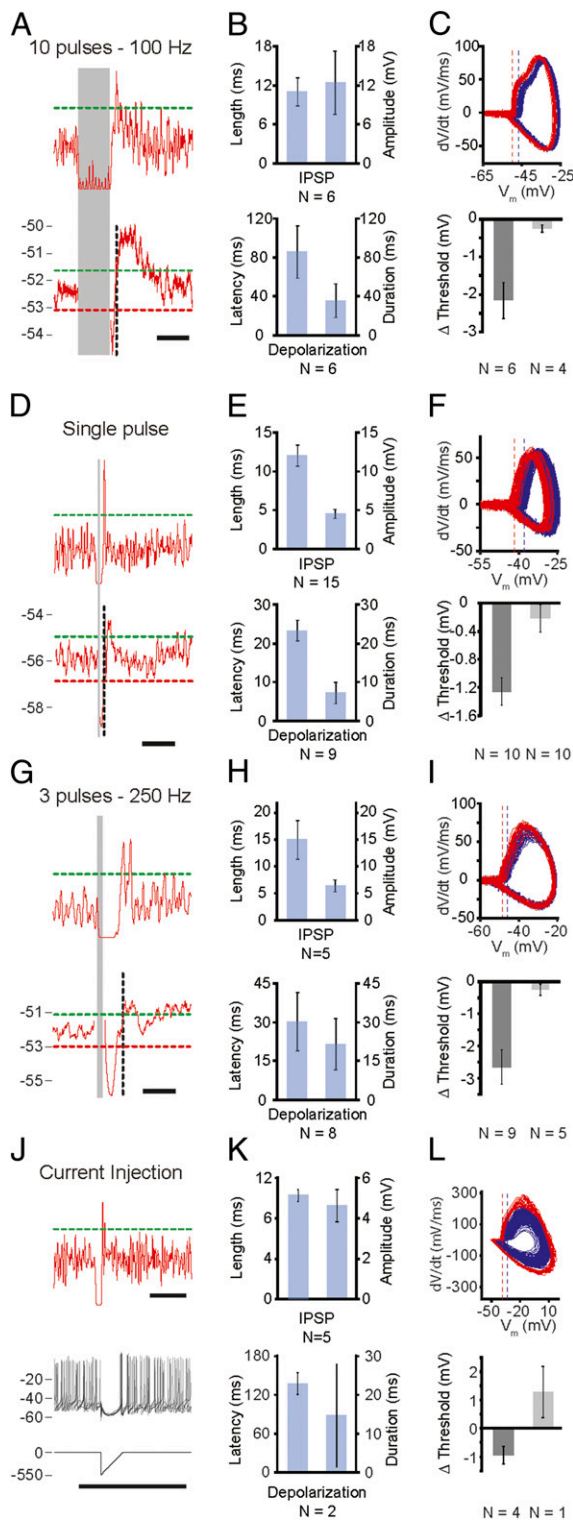


**Fig. 2.** Whole-cell in vivo recordings in CN neurons of ketamine/xylazine-anesthetized mice. (A) Stimulation of the cortex by 10 pulses at 100 Hz (paravermal lobules VI/VII, 100–300  $\mu$ A). (Upper) Gaussian-convolved chance of spiking. The dashed green line indicates a significant increase (+3 SD) of the firing frequency; the gray area indicates the stimulus. (Lower) Average subthreshold membrane potential. The dashed green and red line indicate significantly higher (+3 SD) and lower (–3 SD) membrane-potential thresholds, respectively. The dashed vertical black line indicates the time of the peak in the Gaussian-convolved chance of spiking depicted in the panel above. (Scale bars, 100 ms.) (B) (Upper) Duration and absolute amplitude of the averaged inhibitory postsynaptic potential (IPSP) following the stimulus. (Lower) Latency and dura-

To investigate the potential role of climbing fiber input on CN activity, we simulated climbing fiber activity in the cerebellar cortex by changing our stimulus protocol to three pulses at 250 Hz (cf. ref. 23). This stimulus was successful in evoking three consecutive inhibitory postsynaptic potentials (IPSPs) in 14 CN neurons (Fig. S5A), of which the final amplitude ( $6.4 \pm 1.1$  mV) was not significantly different from that evoked by either 10 pulses at 100 Hz or that evoked by single stimuli ( $P = 0.28$  and  $P = 0.22$ , respectively) (Fig. 2G and H). Following hyperpolarization, the  $V_m$  significantly depolarized in 8 of the 14 responsive CN neurons by  $2.4 \pm 0.5$  mV (relative to the resting  $V_m$  of  $-51.2 \pm 1.8$  mV) (Fig. 2H), which was accompanied by a significant increase in firing frequency in 6 neurons. On the other hand, 9 of the 14 responsive neurons showed significant timed-spiking, which was accompanied by a lower action potential initiation threshold in 4 neurons (Fig. 2I). Thus, in conjunction with the simple spike-like train stimulus (10 pulses at 100 Hz), the complex spike-like stimulus applied to the cerebellar cortex not only elicited timed-spiking activity, but additionally evoked an increased firing frequency in about half of the CN neurons.

These findings raise the question as to whether the timed-spiking activity is a result of stimulus-induced synaptic transmission. We therefore applied hyperpolarizing current injections to five CN neurons, which showed sufficiently low access resistance (38). Current inputs consisted of a hyperpolarizing step (30–550 pA) immediately followed by a repolarizing ramp (10–20 ms) and resulted in an IPSP-like waveform in the recorded neurons (Fig. 2J). These inhibitory postsynaptic current-like inputs were similar to IPSPs following three stimuli at 250 Hz ( $4.6 \pm 0.8$  mV;  $P = 0.23$  and  $9.9 \pm 0.6$  ms;  $P = 0.23$ ) (Fig. 2K) and resulted in well-timed action potential firing in four of five CN neurons for which the initiation threshold was significantly more negative ( $0.95 \pm 0.31$  mV;  $n = 4$ ) (Fig. 2L), with an increased latency ( $P = 0.002$ ), but normal duration ( $P = 0.69$ ) compared with the synaptically evoked rebounds (Fig. 2K). In some cells we blocked inhibitory input in CN neurons, which attenuated the cortically evoked IPSP and abolished rebound activity in these neurons (Fig. S5C). These results indicate that inhibitory input to CN neurons is sufficient to induce timed-spiking activity, as well as subsequent rebound depolarizations that facilitate increased firing frequencies.

**Control of Rebound Activities by the Olivocerebellar Loop.** Quantifying cellular effects downstream in CN neurons following electrical stimulation of a single point in the cerebellar cortex, as described above, probably yields an underestimation, because under physiological conditions CN neurons are activated synchronously by multiple Purkinje cells from potentially non-continuous, sagittal microzones, which receive a common input from electrotonically coupled IO neurons (26, 39). Therefore, we

tion of the averaged, significant depolarization (SI Materials and Methods). (C) (Upper) Membrane potential ( $V_m$ ) re first  $V_m$  derivative ( $dV/dt$ ) indicating the more negative average initiation threshold (dashed lines) for action potentials directly following the stimulus-induced hyperpolarization (rebound; red) and during baseline (blue) for the typical example represented in A. (Lower) Average difference in initiation thresholds ( $\Delta$  threshold) between baseline and rebound action potentials for reacting (Left; dark gray;  $n = 6$ ) and nonreacting (Right; light-gray;  $n = 4$ ) CN neurons. (D–F and G–I) Same as for A to C using a single-pulse stimulus and a three-pulses–250 Hz stimulus train, respectively. (F)  $n = 10$  for both reacting and nonreacting CN neurons. (I)  $n = 9$  for reacting and  $n = 5$  for nonreacting CN neurons. (Scale bars in D and G, 50 ms.) (J) Typical response to an inhibitory postsynaptic current-like current input. (Top) Similar to A. (Middle) Five example traces showing a clear IPSP-like response followed by a timed action potential with a lowered initiation threshold compared with baseline action potentials. (Bottom) A 550 pA hyperpolarizing current injection immediately followed by a repolarizing ramp of 20 ms evoked an IPSP-like waveform in this typical CN neuron. (Scale bar, 100 ms.) (K and L) Similar to B and C. (L)  $n = 4$  for reacting and  $n = 1$  (error bars indicate SEM of recordings) for nonreacting CN neurons.

studied the responses of CN neurons in ketamine-/xylazine-anesthetized rats following graded stimulation of the IO, while recording single-unit activity from excitatory projection neurons in the interposed or lateral CN that were identified by antidromic activation from the red nucleus (Fig. 3) (40).

A total of 66 identified CN neurons responded to IO stimulation with a pause in their firing that started between 5 and 10 ms post-stimulus and ended  $52.0 \pm 4.7$  ms poststimulus. Many of these units ( $n = 31$ ) responded reliably ( $>50\%$ ) with an initial spike before the pause at a latency of 4 to 6 ms poststimulus (Fig. S6). This spike is likely to be triggered by climbing fiber collaterals directly innervating the CN (41). The average firing frequency of 50 units was sig-

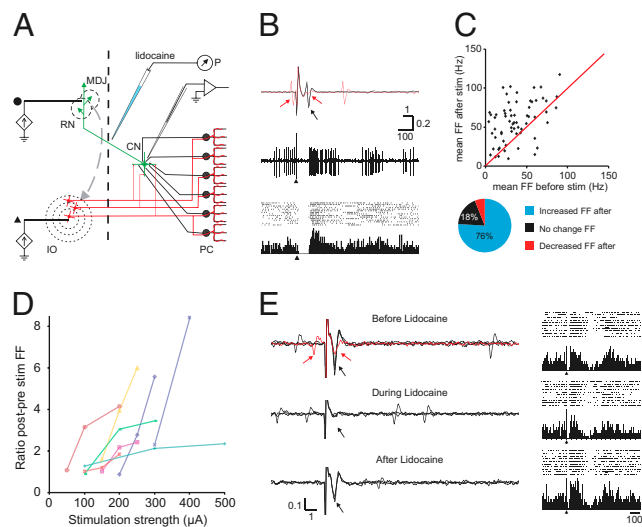


**Fig. 3.** Strong rebound firing in identified CN neurons can be controlled by olivary input. (A) Experimental setup consists of tungsten stimulation electrodes placed in the IO as well as the red nucleus (RN) and mesodiencephalic junction (MDJ) in the midbrain, an injection pipette with lidocaine at the decussation of the superior cerebellar peduncle, and a recording electrode in the CN. Black dot and triangle: stimulus location for traces shown in B and E. P, pressure pump; PC, Purkinje cells. (B) Identification of CN neuron and typical response to IO stimulation. (Top) Three superimposed traces of a CN neuron indicate an antidromic response (black arrow) upon RN-MDJ stimulation at  $150 \mu\text{A}$ . The red sweep shows that a collision with a spontaneous spike blocks the antidromically triggered action potential (red arrows). All 66 analyzed neurons responded in this way to RN-MDJ stimulation. These units did not respond with antidromic activation to IO stimulation, although orthodromic spikes were frequently triggered at short latencies (Fig. S6 E and F). (Middle) IO stimulation (single sweep, single pulse of  $200 \mu\text{A}$  at arrowhead) results in a pause of approximately 60 ms followed by an increase in firing rate. (Bottom) Peristimulus time histogram and accompanying raster plot show the consistency of this phenomenon. (C) (Upper) diagram shows the average firing frequency during the last 250 ms before IO stimulation against the average firing frequency during the first 100 ms after the pause. Firing frequencies were based on averages of  $\geq 15$  sweeps. Red line indicates the unity line. (Lower) Pie-chart indicates the percentage of recorded neurons with statistically significant changes in firing frequency for 50 ms or 250 ms poststimulus. (D) Increasing IO stimulation strength results consistently in increased ratios of post/prestimulus firing frequencies as shown for eight CN neurons. (E) Effect of blocking cerebellar output on poststimulus rebound firing. (Top) identification of a CN neuron by RN stimulation including collision trace (red) and the peristimulus time histogram and raster diagrams to IO stimulation (10 sweeps,  $300 \mu\text{A}$ ). (Middle) responses to RN stimulation of the same unit 5 min after lidocaine (2%, 50–100 nL) injection. Note that antidromic response (and evoked field) had completely disappeared, but that poststimulus rebound activation can still be noted upon the same IO stimulation. (Bottom) responses after recovery from lidocaine (20 min after injection); antidromic responses have returned and IO stimulation results in near-identical responses as seen during blockage of cerebellar output. Horizontal bars indicate time in milliseconds, vertical bars indicate mV.

nificantly increased after the stimulus-induced pause for up to 250 ms. As a group, the average firing frequency more than doubled during this time (Fig. S6A), but the rebound response was especially prominent in units with a spontaneous firing frequency  $<40$  Hz (Fig. S6B). In most of the rebound cases, an increase in stimulus intensity at the IO resulted in a graded enhanced occurrence of the post-stimulus excitatory response (Fig. 3D and Fig. S6C).

Because the onset latency of the rebound (approximately 50 ms) exceeds the duration of the complex spike-induced pause in simple spike firing (10–20 ms) (e.g., see refs. 42–44), the latter phenomenon does not seem to dominate the triggering of the rebound in CN neurons. In addition, these rebounds do not seem to depend on increased activity in long-lasting reverberating loops between CN and precerebellar brainstem nuclei (45, 46), because blocking cerebellar output by injecting lidocaine (50–100 nL) at the decussation of the superior cerebellar peduncle (Fig. 3 A and B) did not have a significant impact on stimulus-induced rebound firing ( $n = 3$ ) (Fig. 3E). Note that in these and other instances, a second increase in firing frequency can be noted (Fig. S6C), which could reflect oscillatory rebound activity in the IO resulting from the synchronous discharge upon stimulation (47, 48). One might speculate that the initial excitatory postsynaptic responses induced by the climbing fiber collaterals contribute indirectly to the rebound responses in CN neurons (Fig. S6 E and F) (49–51), but it is not immediately clear how this short latency response could influence rebound activity occurring  $\geq 40$  ms later. Therefore, it is attractive to hypothesize that rebound firing is mainly caused by the deep and long hyperpolarization induced by synchronously discharged complex spikes.

**Rebound Spiking Occurs Spontaneously.** We have provided evidence that CN neurons can show a significantly increased firing frequency and timed-spiking activity in response to electrical stimulation of the cerebellar cortex or IO, and we now speculate that a hyperpolarization induced by complex spike activities might trigger their rebound firing. If this mechanism is correct, one should also find every few seconds hyperpolarizations that are sufficiently long and that are followed by rebound firing during spontaneous activity, because olivary neurons fire spontaneously at about 1 Hz (52). We therefore aligned in our whole-cell recordings of CN neurons episodes with a significantly more negative  $V_m$  (SI Materials and Methods). In 5 out of 17 CN neurons (Fig. 4A), spontaneous hyperpolarizations ( $-6.6 \pm 0.8$  mV; range  $-3.9$  to

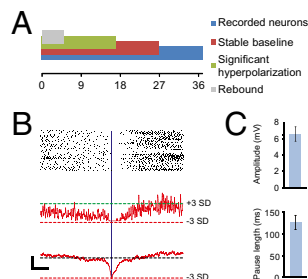


**Fig. 4.** Spontaneous rebound discharges in CN neurons. (A) Summary of analyzed cells, bars are overlapping and represent fractions of the total number of neurons ( $n = 37$ ). (B) Representation of spontaneous rebound discharges of typical CN neuron. (Top) Rasterplot and (Middle) Gaussian-convolved representation of normalized chance of spiking. The dashed horizontal green and red lines indicate a significantly ( $+3$  SD and  $-3$  SD, respectively) increased and decreased chance of spiking, respectively. (Bottom) Accompanying subthreshold membrane potential. Dashed black line indicates the average subthreshold membrane potential ( $-49.9$  mV) and the dashed red line indicates significant hyperpolarizations. [Scale bars, 5 mV (horizontal) and 100 ms (vertical).] All plots are aligned to the significant hyperpolarization (vertical blue line). (C) (Upper) Summary of mean spontaneous IPSP amplitude and (Lower) the accompanying mean length of the pause in firing.

–8.6 mV; relative to the average resting  $V_m$  of  $-53.4 \pm 2.0$  mV (Fig. 4C) occurred that were different from baseline, with a significance level of at least 0.001, and that were also followed by a higher firing frequency (also with a  $P$ -level  $< 0.001$ ), but not timed-spiking activity (Fig. 4B). These spontaneous hyperpolarizations occurred at an average rate of 0.4 Hz and resulted in a pause in CN neuron firing of  $126.7 \pm 41.7$  ms (Fig. 4C), which is compatible with our hypothesis that they are caused by complex spike activities and that they trigger rebound firing.

## Discussion

Our main findings are that stimuli to the cerebellar cortex can result in two separate forms of rebound activity in the CN. These include (i) an increase in firing frequency after an initial pause in firing, which can be induced by train stimuli that mimic either simple spike or complex spike activity; and (ii) timed-spiking activity with no consistent change in the firing rate, which can be induced by single-pulse stimuli. Whole-cell recordings *in vivo* showed that, whereas the increased firing frequency is accompanied by true rebound depolarizations, the timed-spiking activity occurs predominantly before these depolarizations. Despite the effectiveness of the train stimuli applied to the cerebellar cortex, we found the strongest increases in firing frequency when we directly stimulated the IO (41, 49, 53). Moreover, we found spontaneous rebound firing in CN neurons following hyperpolarizations that have temporal characteristics that are compatible with those of complex spike activities. Thus, considering our findings and the overall high level of synchronicity in the olivo-cerebellar modules (54, 55), it is parsimonious to hypothesize that most of the well-timed rebound firing in the CN is induced by activity in the IO.

Our extracellular recordings in the awake, behaving mice showed that, in contrast to a recent report by Alvina et al. (28), we are able to elicit a significant increase in firing frequency in the majority of cells using a stimulus train of 10 pulses at 100 Hz. A major difference between the Alvina study and the present one is their use and choice of anesthetics (isoflurane), which has been shown to affect  $Ca^{2+}$ -channel function (32, 33), as well as activity patterns of cerebellar neurons (56), and thus could well have led to an underestimation of the rebound capabilities of CN neurons (23). One might argue that our use of ketamine/xylazine might have resulted in an overestimation of the rebound capabilities, but there is no evidence for such effects (34–37, 57) and our recordings under anesthesia showed the same type of responses (to both the 10 pulses at 100 Hz and single-pulse stimuli) as those in the awake animals.

Previous studies on the cellular mechanisms underlying rebound capabilities have revealed that specific subtypes of the T-type  $Ca^{2+}$ -channels mediate transient ( $Ca_v3.1$ ) and weak ( $Ca_v3.3$ ) rebound responses (19–21, 58). Although our experiments did not identify whether the recorded neurons expressed each of these  $Ca_v3$ -subtypes, 3 of 27 CN neurons recorded in the awake mice showed considerably larger increases in their firing rates than others, which might implicate that these neurons express  $Ca_v3.1$  T-type  $Ca^{2+}$ -channels. In addition to the classification of CN neurons based upon their rebound capabilities, our recordings also allow the comparison of the rebound capabilities upon the baseline activities; by projecting the rebound responses for each responsive neuron on the baseline activities of all recorded neurons, we found, for example, that CN neurons that fire spikes relatively slowly and highly regularly have a remarkably low susceptibility to rebound activity (Fig. S1). It remains to be elucidated, however, whether such particular firing patterns characterize a specific type of neuron: that is, GABAergic, glycinergic, or glutamatergic CN neurons (also see refs. 4, 14).

In addition to characterizing the physiologically relevant spiking patterns in CN neurons, the present study was also designed to dissociate between the rebound responses to simple spike-like train

stimuli, complex spike-like stimuli, and single-pulse stimuli. Our results show several remarkable comparisons between the individual response types. First, both simple spike-like and complex spike-like train stimuli induce not only actual rebound depolarizations that are accompanied by increased firing rates, but also induce action potential firing before these rebound depolarizations. This pattern of rebound activities was recently also described in an *in vitro* study that revealed rebound depolarizations induced by action potential-mediated high-voltage activated  $Ca^{2+}$ -channel activation (23). Second, our results show that in response to single-pulse stimuli, timed-spiking activity prevails even when rebound depolarizations are mostly absent, indicating that the underlying mechanisms are not yet fully elucidated. Third, the responses to simple spike- and complex spike-like train stimuli overlapped extensively. One may argue this is because of a possibly detrimental effect of the reported axonal cut-off frequency for propagation of action potentials along Purkinje cell axons (59, 60). However, such effect seems unlikely because IPSPs could be detected in response to both the 250-Hz and 100-Hz stimulus trains (Fig. S5). Instead, we propose that the electrical stimulation of the cerebellar cortex overall was suboptimal, because optimal increases may require activation of many Purkinje cells that project to a single CN neuron, and which are organized in non-continuous sagittal zones (61). The current study provides two results that confirm this hypothesis: direct olivary stimulations induced the most vigorous increases in firing frequencies, and rebound activities were observed following IPSPs during spontaneous CN neuron activity (26, 62). The fact that this spontaneous rebound activity is found at lower frequencies than that of spontaneously occurring complex spikes suggests that only during specific situations, possibly when the electrotonic coupling and therefore the synchrony within the olive is sufficient, this rebound activity may occur.

Rebound firing has been shown to be a likely candidate to facilitate  $Ca^{2+}$ -influx inducing plasticity of mossy-fiber collaterals in CN neurons (23, 63, 64). For example, strong increases in the CN firing rate might come about when a subject has to react quickly to unexpected events or show learning-dependent timing, which both require a well-coupled olivary network (46). Timed-spiking activity on the other hand might have a role in conducting a timing signal downstream. Indeed, neurons in the ventro-anterior and ventrolateral complex of the thalamus, which receive a direct, monosynaptic input from the excitatory neurons in the interposed nucleus, are known to show an all-or-none response to single-pulse stimulations to these CN (65, 66). Thus, single well-timed spikes in thalamic projection neurons could be an effective measure to transmit, for example, the timing of a motor command (15, 67, 68). Still, even though the synchrony level among simple spike activities can, under particular circumstances, be just as high as that among complex spike activities (69), and single pulses may have detectable effects downstream (65), the present data show that the impact on rebound activity is much more pronounced when synchrony is induced via the complex spike activities: that is, the climbing fiber pathway originating in the IO (49).

## Materials and Methods

Awake and anesthetized adult C57BL/6 mice and Wistar rats were used for both extracellular and whole-cell patch-clamp recordings using borosilicate glass electrodes. We recorded the responses to electrical activation of the cerebellar cortex and IO using train and single pulse stimuli. Data are represented as mean  $\pm$  SEM unless stated otherwise. For a complete detailed description, see *SI Materials and Methods*.

**ACKNOWLEDGMENTS.** The authors thank Ing. J. van der Burg for excellent technical assistance and other laboratory members for helpful discussions. This work was supported by The Netherlands Organization for Scientific Research -Earth and Life Sciences (F.E.H. and C.I.D.Z.), NeuroBisik (C.I.D.Z.), Prinses Beatrix Fonds (C.I.D.Z.), and SENSORimotor Structuring of Perception and Action for Emergent Cognition (C.I.D.Z.).

1. Pugh JR, Raman IM (2009) Nothing can be coincidence: Synaptic inhibition and plasticity in the cerebellar nuclei. *Trends Neurosci* 32:170–177.
2. De Zeeuw CI, Berrebi AS (1995) Postsynaptic targets of Purkinje cell terminals in the cerebellar and vestibular nuclei of the rat. *Eur J Neurosci* 7:2322–2333.
3. Teune TM, van der Burg J, van der Moer J, Voogd J, Ruigrok TJ (2000) Topography of cerebellar nuclear projections to the brain stem in the rat. *Prog Brain Res* 124:141–172.
4. Uusisaari M, Knöpfel T (2008) GABAergic synaptic communication in the GABAergic and non-GABAergic cells in the deep cerebellar nuclei. *Neuroscience* 156:537–549.
5. Chan-Palay V (1977) *Cerebellar Dentate Nucleus: Organization, Cytology and Transmitters* (Springer-Verlag, Berlin).
6. de Zeeuw CI, Berrebi AS (1996) Individual Purkinje cell axons terminate on both inhibitory and excitatory neurons in the cerebellar and vestibular nuclei. *Ann N Y Acad Sci* 781:607–610.
7. Van der Want JJ, Wiklund L, Guegan M, Ruigrok T, Voogd J (1989) Anterograde tracing of the rat olivocerebellar system with *Phaseolus vulgaris* leucoagglutinin (PHA-L). Demonstration of climbing fiber collateral innervation of the cerebellar nuclei. *J Comp Neurol* 288:1–18.
8. Aizenman CD, Linden DJ (1999) Regulation of the rebound depolarization and spontaneous firing patterns of deep nuclear neurons in slices of rat cerebellum. *J Neurophysiol* 82:1697–1709.
9. Alviña K, Khodakhah K (2008) Selective regulation of spontaneous activity of neurons of the deep cerebellar nuclei by N-type calcium channels in juvenile rats. *J Physiol* 586:2523–2538.
10. Jahnsen H (1986) Electrophysiological characteristics of neurones in the guinea-pig deep cerebellar nuclei in vitro. *J Physiol* 372:129–147.
11. Llinás R, Mühlethaler M (1988) Electrophysiology of guinea-pig cerebellar nuclear cells in the in vitro brain stem-cerebellar preparation. *J Physiol* 404:241–258.
12. Raman IM, Gustafson AE, Padgett D (2000) Ionic currents and spontaneous firing in neurons isolated from the cerebellar nuclei. *J Neurosci* 20:9004–9016.
13. Thach WT (1968) Discharge of Purkinje and cerebellar nuclear neurons during rapidly alternating arm movements in the monkey. *J Neurophysiol* 31:785–797.
14. Uusisaari M, Obata K, Knöpfel T (2007) Morphological and electrophysiological properties of GABAergic and non-GABAergic cells in the deep cerebellar nuclei. *J Neurophysiol* 97:901–911.
15. Kistler WM, De Zeeuw CI (2002) Dynamical working memory and timed responses: The role of reverberating loops in the olivo-cerebellar system. *Neural Comput* 14:2597–2626.
16. Masuda N, Amari S (2008) A computational study of synaptic mechanisms of partial memory transfer in cerebellar vestibulo-ocular-reflex learning. *J Comput Neurosci* 24:137–156.
17. Wetmore DZ, Mukamel EA, Schnitzer MJ (2008) Lock-and-key mechanisms of cerebellar memory recall based on rebound currents. *J Neurophysiol* 100:2328–2347.
18. Wulff P, et al. (2009) Synaptic inhibition of Purkinje cells mediates consolidation of vestibulo-cerebellar motor learning. *Nat Neurosci* 12:1042–1049.
19. Alviña K, Ellis-Davies G, Khodakhah K (2009) T-type calcium channels mediate rebound firing in intact deep cerebellar neurons. *Neuroscience* 158:635–641.
20. Molineux ML, et al. (2006) Specific T-type calcium channel isoforms are associated with distinct burst phenotypes in deep cerebellar nuclear neurons. *Proc Natl Acad Sci USA* 103:5555–5560.
21. Molineux ML, et al. (2008) Ionic factors governing rebound burst phenotype in rat deep cerebellar neurons. *J Neurophysiol* 100:2684–2701.
22. Muri R, Knöpfel T (1994) Activity induced elevations of intracellular calcium concentration in neurons of the deep cerebellar nuclei. *J Neurophysiol* 71:420–428.
23. Zheng N, Raman IM (2009) Ca currents activated by spontaneous firing and synaptic disinhibition in neurons of the cerebellar nuclei. *J Neurosci* 29:9826–9838.
24. Eccles JC, Llinás R, Sasaki K (1966) Parallel fibre stimulation and the responses induced thereby in the Purkinje cells of the cerebellum. *Exp Brain Res* 1:17–39.
25. Ito M, Simpson JI (1971) Discharges in Purkinje cell axons during climbing fiber activation. *Brain Res* 31:215–219.
26. Llinás R, Sasaki K (1989) The functional organization of the olivo-cerebellar system as examined by multiple Purkinje cell recordings. *Eur J Neurosci* 1:587–602.
27. Mathy A, et al. (2009) Encoding of oscillations by axonal bursts in inferior olive neurons. *Neuron* 62:388–399.
28. Alviña K, Walter JT, Kohn A, Ellis-Davies G, Khodakhah K (2008) Questioning the role of rebound firing in the cerebellum. *Nat Neurosci* 11:1256–1258.
29. Hoebeek FE, et al. (2005) Increased noise level of Purkinje cell activities minimizes impact of their modulation during sensorimotor control. *Neuron* 45:953–965.
30. Gauck V, Jaeger D (2000) The control of rate and timing of spikes in the deep cerebellar nuclei by inhibition. *J Neurosci* 20:3006–3016.
31. Rowland NC, Jaeger D (2005) Coding of tactile response properties in the rat deep cerebellar nuclei. *J Neurophysiol* 94:1236–1251.
32. Study RE (1994) Isoflurane inhibits multiple voltage-gated calcium currents in hippocampal pyramidal neurons. *Anesthesiology* 81:104–116.
33. Todorovic SM, Lingle CJ (1998) Pharmacological properties of T-type Ca<sup>2+</sup> current in adult rat sensory neurons: Effects of anticonvulsant and anesthetic agents. *J Neurophysiol* 79:240–252.
34. Hevers W, Hadley SH, Lüddens H, Amin J (2008) Ketamine, but not phencyclidine, selectively modulates cerebellar GABA(A) receptors containing alpha6 and delta subunits. *J Neurosci* 28:5383–5393.
35. Devor A, Fritschy JM, Yarom Y (2001) Spatial distribution and subunit composition of GABA(A) receptors in the inferior olivary nucleus. *J Neurophysiol* 85:1686–1696.
36. Pirker S, Schwarzer C, Wieselthaler A, Sieghart W, Sperk G (2000) GABA(A) receptors: Immunocytochemical distribution of 13 subunits in the adult rat brain. *Neuroscience* 101:815–850.
37. Bengtsson F, Jörntell H (2007) Ketamine and xylazine depress sensory-evoked parallel fiber and climbing fiber responses. *J Neurophysiol* 98:1697–1705.
38. Margrie TW, Brecht M, Sakmann B (2002) In vivo, low-resistance, whole-cell recordings from neurons in the anaesthetized and awake mammalian brain. *Pflügers Arch* 444:491–498.
39. De Zeeuw CI, et al. (1998) Microcircuitry and function of the inferior olive. *Trends Neurosci* 21:391–400.
40. Haroian AJ, Massopust LC, Young PA (1981) Cerebellothalamic projections in the rat: An autoradiographic and degeneration study. *J Comp Neurol* 197:217–236.
41. Kitai ST, McCreag RA, Preston RJ, Bishop GA (1977) Electrophysiological and horseradish peroxidase studies of precerebellar afferents to the nucleus interpositus anterior. I. Climbing fiber system. *Brain Res* 122:197–214.
42. Sato Y, Miura A, Fushiki H, Kawasaki T (1992) Short-term modulation of cerebellar Purkinje cell activity after spontaneous climbing fiber input. *J Neurophysiol* 68:2051–2062.
43. Simpson JI, Wylie DR, De Zeeuw CI (1996) On climbing fiber signals and their consequence(s). *Behav Brain Sci* 19:384–398.
44. Sato Y, Miura A, Fushiki H, Kawasaki T (1993) Barbiturate depresses simple spike activity of cerebellar Purkinje cells after climbing fiber input. *J Neurophysiol* 69:1082–1090.
45. Tsukahara N, Bando T, Murakami F, Oda Y (1983) Properties of cerebello-precerebellar reverberating circuits. *Brain Res* 274:249–259.
46. Van Der Giessen RS, et al. (2008) Role of olivary electrical coupling in cerebellar motor learning. *Neuron* 58:599–612.
47. Khosrovani S, Van Der Giessen RS, De Zeeuw CI, De Jeu MT (2007) In vivo mouse inferior olive neurons exhibit heterogeneous subthreshold oscillations and spiking patterns. *Proc Natl Acad Sci USA* 104:15911–15916.
48. Ruigrok TJ, Voogd J (1995) Cerebellar influence on olivary excitability in the cat. *Eur J Neurosci* 7:679–693.
49. Ruigrok TJ (1997) Cerebellar nuclei: The olivary connection. *Prog Brain Res* 114:167–192.
50. Ruigrok TJ, Voogd J (2000) Organization of projections from the inferior olive to the cerebellar nuclei in the rat. *J Comp Neurol* 426:209–228.
51. Audinat E, Gähwiler BH, Knöpfel T (1992) Excitatory synaptic potentials in neurons of the deep nuclei in olivo-cerebellar slice cultures. *Neuroscience* 49:903–911.
52. Armstrong DM (1974) Functional significance of connections of the inferior olive. *Physiol Rev* 54:358–417.
53. Rowland NC, Jaeger D (2008) Responses to tactile stimulation in deep cerebellar nucleus neurons result from recurrent activation in multiple pathways. *J Neurophysiol* 99:704–717.
54. Lang EJ, Llinás R, Sugihara I (2006) Isochrony in the olivocerebellar system underlies complex spike synchrony. *J Physiol* 573:277–279, author reply 281–282.
55. Sugihara I, Lang EJ, Llinás R (1993) Uniform olivocerebellar conduction time underlies Purkinje cell complex spike synchronicity in the rat cerebellum. *J Physiol* 470:243–271.
56. Schonewille M, et al. (2006) Purkinje cells in awake behaving animals operate at the upstate membrane potential. *Nat Neurosci* 9:459–461, author reply 461.
57. Laurie DJ, Seeburg PH, Wisden W (1992) The distribution of 13 GABAA receptor subunit mRNAs in the rat brain. II. Olfactory bulb and cerebellum. *J Neurosci* 12:1063–1076.
58. Tadayonnejad R, Mehaffey WH, Anderson D, Turner RW (2009) Reliability of triggering postinhibitory rebound bursts in deep cerebellar neurons. *Channels (Austin)* 3:149–155.
59. Khaliq ZM, Raman IM (2005) Axonal propagation of simple and complex spikes in cerebellar Purkinje neurons. *J Neurosci* 25:454–463.
60. Monsivais P, Clark BA, Roth A, Häusser M (2005) Determinants of action potential propagation in cerebellar Purkinje cell axons. *J Neurosci* 25:464–472.
61. Pijpers A, Voogd J, Ruigrok TJ (2005) Topography of olivo-cortico-nuclear modules in the intermediate cerebellum of the rat. *J Comp Neurol* 492:193–213.
62. Cheron G, et al. (2004) Inactivation of calcium-binding protein genes induces 160 Hz oscillations in the cerebellar cortex of alert mice. *J Neurosci* 24:434–441.
63. Pugh JR, Raman IM (2006) Potentiation of mossy fiber EPSCs in the cerebellar nuclei by NMDA receptor activation followed by postinhibitory rebound current. *Neuron* 51:113–123.
64. Pugh JR, Raman IM (2008) Mechanisms of potentiation of mossy fiber EPSCs in the cerebellar nuclei by coincident synaptic excitation and inhibition. *J Neurosci* 28:10549–10560.
65. Sawyer SF, Young SJ, Groves PM, Tepper JM (1994) Cerebellar-responsive neurons in the thalamic ventroanterior-ventrolateral complex of rats: In vivo electrophysiology. *Neuroscience* 63:711–724.
66. Uno M, Yoshida M, Hirota I (1970) The mode of cerebello-thalamic relay transmission investigated with intracellular recording from cells of the ventrolateral nucleus of cat's thalamus. *Exp Brain Res* 10:121–139.
67. Koekkoek SK, et al. (2005) Deletion of FMR1 in Purkinje cells enhances parallel fiber LTD, enlarges spines, and attenuates cerebellar eyelid conditioning in Fragile X syndrome. *Neuron* 47:339–352.
68. Mauk MD, Medina JF, Nores WL, Ohyama T (2000) Cerebellar function: Coordination, learning or timing? *Curr Biol* 10:R522–R525.
69. De Zeeuw CI, Koekkoek SK, Wylie DR, Simpson JI (1997) Association between dendritic lamellar bodies and complex spike synchrony in the olivocerebellar system. *J Neurophysiol* 77:1747–1758.